The functional connectivity of the human claustrum according to the Human Connectome Project database

Lluviana Rodríguez-Vidal[1], Sarael Alcauter[1], Fernando A Barrios[1,*]

[1] Universidad Nacional Autónoma de México, Instituto de Neurobiología, Querétaro, QRO, México.

***Corresponding author:**
Fernando A Barrios, PhD.
Universidad Nacional Autónoma de México, Instituto de Neurobiología
Blvd. Juriquilla 3001, Juriquilla, Querétaro, Querétaro 76230, México
fbarrios@unam.mx
Tel +52(442)238-1053

Total number of words (excluding title page, tables and figure legends): 3965

Abstract

The claustrum is an irregular and fine sheet of grey matter in the basolateral telencephalon present in almost all mammals. The claustrum has been the object of several studies using animal models and more recently in human beings using neuroimaging. It has been involved in cognition and disease such as fear recognition, suppression of natural urges, multisensory integration, conceptual integration, seizures, multiple sclerosis and Parkinson´s disease. Nevertheless, the function of the claustrum still remains unclear. We present a high resolution functional connectivity study of the claustrum in order to identify its main networks. Resting state functional and anatomical MRI data from 100 healthy subjects were analyzed; taken from the Human Connectome Project (HCP, NIH Blueprint: The Human Connectome Project), with 2x2x2 mm^3 voxel resolution, equivalent to the high resolution tractography studies. Positive functional connectivity was found ($p<0.05$, FDR corrected) between the claustrum and the insula, anterior cingulate cortex, pre-central and postcentral gyrus, superior temporal gyrus and subcortical areas. Our findings coincide with the results previously reported in both animal models and studies with humans. Showing the claustrum as a well connected structure not only structurally but also functionally. Evidencing the claustrum as a node participating in different neural networks.

Keywords: Brain connectivity, resting state, HCP, insula, thalamus, cingulate cortex

Introduction

The claustrum is an irregular and fine sheet of grey matter in the basolateral telencephalon present in almost all mammals. The claustrum is separated from the insular cortex by the extreme capsule and medially from the lentiform nucleus by the external capsule[1–7]. Figure 1 shows in an axial view the anatomical location of the human claustrum. Research in humans using diffusion tensor imaging (DTI) have revealed cortical connections with the claustrum, which possesses projections to A) prefrontal cortex, BA 8, 9, 10, 11, 12 and 34; B) visual cortex, BA 17, 18, 19 and 39; C) sensoriomotor cortex, BA 7, 5, 1/2/3, 4, 6 and 8; and D) language areas BA 44, 45 and 31; as well as with orbitofrontal cortex, temporal cortex, basal ganglia and amygdala[3,7,8] using DTI in 100 healthy subjects, Torgerson et al.[8] found that the claustrum has the highest connectivity in the brain by regional volume. The literature about the claustrum – including studies in animal model and in humans – has evidenced the vast anatomical connections between the claustrum and the entire cerebral cortex as well as with the subcortical structures[1–4,6–9].

Based on its cellular composition and wide structural connectivity, the claustrum has been described as a "cornerstone of sensory integration"[1]. In a similar way,[2] proposed the claustrum as a crucial component integrating motor and sensory information coming from different modalities to assemble them in a single experience; in an analogy used by Crick and Koch, the claustrum is as an orchestra conductor, "[w]ithout the conductor, the players can still play but they fall increasingly out of synchrony with each other."[2]; actually, this proposal has been one of the most influential in the claustrum literature. In addition, the claustrum has been proposed as a relevant structure in the segregation of attention[4,6].

Claustrum have been involved in cognitive process such as fear recognition, suppression of natural urges, multisensory integration and conceptual integration. The involvement of the claustrum in such processes is the result of a different research question more than the question of the function of claustrum by itself[10–13]. Although it is rarely reported in the medical literature the selective lesion of the claustrum; the claustrum has been involved in disease such as seizures, multiple sclerosis, Parkinson´s diseases, disruption of consciousness, auditory hallucinations and delusions[14–17].

Resting-state functional connectivity (RSFC) has proved to be a useful tool to characterize the functional communication of specific brain areas. Examining resting state functional connectivity allows us to determine the correlation between the spontaneous activity of brain areas that are anatomically separated, observing if there is functional communication between brain regions, specifically, is defined as the temporal dependency of neuronal activation patterns of anatomically

separated brain regions[18]. A recent study in humans using functional magnetic resonance imaging (fMRI) shown the functional connectivity between the claustrum and anterior cingulate cortex, prefrontal, visual and parietal cortices[19]. They also reported functional connectivity between the claustrum and posterior cingulate cortex, precuneus, angular gyrus, cuneus, visual cortex, and sensorimotor cortex, as well as with subcortical structures such as thalamus and nucleus accumbens among others, according to this study, their results suggest the association of the claustrum with cognitive control. Nevertheless, in order to have a clear or complete understanding on the function of the claustrum beyond of the theoretical proposals[2,4] we will require an accumulation of many studies to find certitude about our conclusions.

One of the most challenging issues to study the human claustrum is its intricated anatomical location and its irregular form. Technical constrains have limited the detailed study of the claustrum. We propose to approach these challenges by assessing the whole brain resting state functional connectivity of the claustrum using the high-resolution WU-Minn Human Connectome Project (HCP) dataset, which, differs qualitatively from the standard neuroimgen data, due to its higher spatial and temporal resolution and differing distortion. The functional datasets were acquired with a spatial resolution of 2 mm isotropic and a temporal resolution of 0.7 s at 3T, which in a non usual high spatial or temporal resolution for whole brain coverage, Van[20–24]. In this study, we aimed to explore, by a seed driven analysis, the resting-state functional connectivity of the human claustrum based on a large cohort of healthy subjects.

Materials and methods

Subjects

The study included data from 100 healthy young adults with ages between 22 and 35 years old, representing healthy subjects who have passed the age of major neurodevelopmental changes and have not onset the age of degenerative changes. Subjects were selected from the 1200 adult subject public WU-Minn Human Connectome Project (HCP NIH Blueprint: The Human Connectome Project, https://www.humanconnectome.org/study/hcp-young-adult/data-releases)[22]. HCP excluded subjects having history of psychiatric, neurological or neurodevelopmental disorder or substance abuse. A full and detailed description of the recruitment criteria is provided by Van Essen et al.,[22,23]. Our sample from the HCP data was restricted to 100 unrelated subjects with complete resting-state functional magnetic resonance imaging (rfMRI) and anatomical MRI datasets. The full informed consent from all

participants was obtained by the WU-Minn HCP Consortium. The protocols of the data acquisition and distribution of the dataset complied with the Code of Ethics of the World Medical Association[23].

Image acquisitions and preprocessing

The HCP acquired anatomical and resting-state functional MRI data at Washington University using a customized Siemens 3T "Connectome Skyra" with a standard 32-channel head coil. Structural dataset acquisitions included high resolution T1-weighted (T1w) and T2-weighted (T2w) images with 0.7 mm isotropic resolution, FOV = 224x224 mm, matrix = 320, 256 sagittal slices in a single slab TR = 2400 ms, TE = 2.14 ms, TI = 1000 ms, FA = 8°. Resting-state fMRI were acquired at 2 mm isotropic resolution, TR=720ms, TE = 33.1 ms, slice thickness of 2.0 mm, 72 slices. Uğurbil et al.,[24] and Glasser et al.,[20] provide a full and detailed description of the HCP acquisition protocols. We include in our study the HCP dataset preprocessed by the HCP which due its higher spatial and temporal resolutions and differing distortions must be processed differently from standard neuroimaging data in order to achieve optimal results.[20,24]. Pipelines developed by HCP include spatial distortion correction, motion correction, spatial registration and normalization to MNI coordinates, highpass filtering (cutoff=2,000s) and denoising of rfMRI data. In addition, we use as confound regressors BOLD signal from the white matter and cerebrospinal fluid (CSF) mask and band-pass filtering (0.01 – 0.08 Hz). In order to minimize potential signal contamination from adjacent structures, the timeseries data from regions of interest (ROIs) were not smoothed. The linear regression and filtering were carried out using *conn toolbox* (V18b, Functional connectivity toolbox, NITRC)[25], SPM 12 software[26] and matlab R2019a (https://www.mathworks.com). The analysis was executed using the standard resting state pipeline included in *conn* to simplified posterior reproducibility.

Mask of claustrum and functional connectivity

The T1 anatomical volumes were used to manually delineate right and left claustrum masks for each subject, in an axial plane, in a superior-to-inferior manner to identify the body of the claustrum and edited in the coronal and sagittal plane for accuracy. We transformed them into the rfMRI space, spatially averaged the claustrum masks and established the threshold (0.1) of the mask to transform it into a binary mask. All these processes were carried on through the FMRIB software Library (FSL) tools v5.0. The averaged claustrum masks constituted our seeds to perform a seed-based functional connectivity analysis.

High resolution functional connectivity maps were estimated using the Conn toolbox (V18b, Functional connectivity toolbox, NITRC)[25], SPM 12 software[26] and matlab R2019a. Pearson correlation

coefficients were calculated within each subject in MNI space taking the seed time course and the time course of all other voxels (seed-to-voxel analysis) or the cortical/subcortical structures (seed-to-ROI analysis). The resultant correlation coefficient maps were converted to normally distributed scores using Fisher transform to permit a second-level analysis, in which, a one-sample t-test was performed. The resultant connectivity maps were corrected at map level $p<0.05$ using False Discovery Rate (FDR).

Results

The claustrum was delimited by our averaged mask whose dimensions are 31mm x 1 mm x 17 mm. We closely coincide with the dimension described by Kapakin[5]; figure 2 shows on an axial view the average mask used in the analysis, our effective claustrum ROI, was estimated from the intersection of all subjects´ claustrum.

In a seed-to-voxel analysis, we identified functional connectivity of the left claustrum ($p<0.05$ p-FDR corrected) with precentral gyrus, postcentral gyrus, insular cortex, superior temporal gyrus, supramarginal gyrus, opercular cortex, frontal cortex and anterior cingulate cortex (Figure 3, Supplementary Material, Table SS1). We found functional connectivity between the right calustrum and precentral gyrus, postcentral gyrus, insular cortex, temporal cortex supramarginal gyrus, opercular cortex, frontal cortex, cingulate gyrus and occipital cortex (Figure 4, Supplementary Material, Table SS2).

We performed a seed-to-ROI analysis using as seeds the right and left claustrum masks and 132 ROIs combining FSL Harvard-Oxford atlas cortical and subcortical areas and AAL atlas cerebellar areas, the analysis was carried on using Conn toolbox. The results were thresholded $p<0.05$ p-FDR corrected at seed-level. We obtained a positive correlation between the left claustrum and left insular cortex, pre and postcentral left gyrus, left opercular cortex, left temporal cortex, left supplementary motor area (SMA), anterior cingulate cortex, (Figure 5, Table I) left and right putamen, hippocampus and amygdala (Table III), we found also functional connectivity between the left claustrum and cerebellum (Figure 6, Table V).

In same way when using the right claustrum as seed we obtained positive functional connectivity with right insular cortex, right opercular cortex, pre and postcentral right gyrus, anterior cingulate cortex, right temporal cortex, right supplementary motor area, right frontal cortex, right parietal cortex, (Figure 5, Table II) right putamen, right hippocampus, amygdala and cerebellum, (Figure 6, Table IV, VI).

Finally, functional connectivity was also found with network cortical ROIs. The claustra are functionally connected with nodes of the salience network, including anterior insula, rostral prefrontal cortex (RPFC), anterior cingulate cortex, supramarginal gyrus, language network whose areas are the inferior frontal gyrus (IFG), posterior superior temporal gyrus(pSTG), areas of the dorsal attention network, such frontal eye field (FEF), the intraparietal sulcus (IPS). The superior and lateral areas pertaining to the sensoriomotor network, and visual areas such as medial and lateral occipital visual area (Figure 7, Table VII, VIII).

Discussion

Here, we carried out a seed-driven functional connectivity analysis in a sample of 100 healthy subjects, we found that the human claustrum is widely connected with cortical and subcortical brain areas. Left and right claustrum are mainly connected with insular cortex, precentral gyrus, opercular cortex, supplementary motor area, anterior cingulate cortex, paracingulate cortex, frontal cortex, temporal and occipital cortex, putamen, hippocampus, amygdala and cerebellar areas. We found functional connectivity with specific nodes of the characterized brain networks such as salience, sensori-motor, language, dorsal attention, default mode, frontoparietal, visual and cerebellar anterior, which imply that the claustrum is not only well connected structurally but also functionally.

Our findings reveal that the claustrum maintains a functional connectivity with regions of the salience network, this could be justified not only due to the anatomical closeness of the claustrum with the insula, but also because they share ontogeny. Pirone *et al*.,[27] using immunohistochemistry technique and samples of insular and temporal subunits of the human claustrum, revealed that the claustrum share ontogeny with the insular cortex, but not with putamen. Additionally, Remedios et al.,[28] analyzed the neurons located in the auditory zone of the primate claustrum and arrived to the conclusion that the clausturm detects the occurrence of novel or salient stimulus.

On the other hand, we found functional connectivity between the claustrum and sensori-motor areas, visual areas, anterior cingulate cortex, frontal cortex, which is consistent with previous research that the claustrum participate in cognition. Coactivation of the claustrum has been previously reported in different cognitive processes such as integration of sensory signal across the tactile and visual modalities, multisensory integration of conceptually related common objects, suppression of natural urges, retrieval fluency, cognitive control and task switching[10–13,19,29]. Claustral activation is reported in a fMRI study about the neuronal bases of the integration of auditory and visual stimuli, which, were

conceptually related (congruent). The authors of this study concluded that the contribution of the claustrum was related to the congruence of stimuli, not only to the matching of these[13].

To date, there are several hypotheses about the function of the claustrum; one of the most important in this regard was proposed by Crick and Koch[2], who proposed the claustrum as an important hub which integrates stimuli from different sensory modalities. Hadjikhani et al.,[11] researching neural bases of tactile–visual cross-modal transfer of shape in humans using neuroimaging, found that the claustrum has an important role in cross-modal matching. Their results suggest that the cross-modal adaptation is associated with multimodal converging brain areas such as anterior cingulate cortex, inferior parietal lobe, superior and mid temporal cortex, dorsolateral prefrontal cortex and insular cortex. Banati et al.,[10] also found activation by tactile-visual stimuli in anterior cingulate cortex, dorsolateral prefrontal cortex, mid and superior temporal cortex and insula cortex. Our findings are consistent with these previous studies, anterior cingulate cortex, superior, temporal cortex and insular cortex are functionally connecting with the claustrum.

On the other hand, another important hypothesis about the function of the claustrum is related to segregation of attention[4,6]. The claustrum is considered as a hub for attention, according to this model, the prefrontal cortex modules to the claustrum in a top down process and the output of the claustrum modules the cortical representation of the sensory modalities. The claustrum controls which cortical output will be attended amplifying the preferred modality and reducing the other ones. This process would be modulated by additional subcortical inputs related to the context and emotion hippocampus and amygdala respectively. Our results are compatible with this model, since we found a positive correlation between the claustrum and the prefrontal cortex, anterior cortex cingulate, pre and postcentral gyrus, amygdala and hippocampus, which, according to the model of Goll et al.[4] are implied in the segregation of attention[4].

We are confident that our study could contribute to the understanding of this thin but well connected structure: the claustrum. The use of the high quality HCP datasets provide us of advantages to our study, because of its high spatial and temporal resolution; and to the standardized preprocessing accomplished by the HCP members. Additionally, the age range chosen (22-35 years-old) permit an unbiased analyses due to it represent healthy adults who are not experimenting the major neurodevelopmental changes nor neurodegenerative changes[22]. Nevertheless, our research does not include the claustrum in action, which implies a limitation in order to have greater certainty about its function. Also, we focus on present the connectivity of the average claustrum, we did not consider

handedness or gender related effects. Despite the fact that we use high-resolution images, the structure of the claustrum itself is fine, irregular and its location complicates a finer analysis.

In conclusion, the claustrum is a highly connected brain structure, hardly to study due its anatomical location and irregular form. Neuroimaging offers a powerful tool to explore its function non-invasively, despite its limited resolution. Making use of open access high resolution datasets, we present an approximation of the resting-state functional connectivity of the claustrum, which maintains positive functional connectivity not only with cortical brain areas, but subcortical and different brain networks such as salience, sensorimotor, language, and attention.

Acknowledgements

We thank the 'Programa de Doctorado en Ciencias Biomédicas' of the 'Universidad Nacional Autónoma de México (UNAM)' and the Consejo Nacional de Ciencia y Tecnología, (CONACYT) for the doctoral fellowship no. 477467 (Ll R-V) supported by the National Council of Science and Technology, Mexico (Consejo Nacional de Ciencia y Tecnología, CONACYT) and the PAPIIT program DGAPA-UNAM for the grant IN202119. The authors thankfully acknowledge the imaging resources and support provided by the "Laboratorio Nacional de Imagenología por Resonancia Magnética", CONACyT network of national laboratories. LlR-V is grateful to N. Aranda-López for her administrative support. We are also grateful to M.Sc. Leopoldo González-Santos and Dr. Erick H. Pasaye for technical support and Dr. M.C. Jeziorski for his revision of the manuscript.

Author contributions

LlR-V, SA and FAB developed the study concept, contributed to the study design. Data analysis and interpretation was performed by LlR-V, SA and FAB. All work was done under the supervision of FAB. LlR-V wrote the manuscript draft. All authors provided critical revisions and approved the final version of the manuscript.

Competing interests

The authors declare no competing interests.

Data availability

All data related to this research is accessible at the Human Connectome Project site https://www.humanconnectome.org/study/hcp-young-adult/data-releases

References

1. Edelstein, L. R. & Denaro, F. J. The claustrum: a historical review of its anatomy, physiology, cytochemistry and functional significance. *Cell Mol Biology Noisy-le-grand France* **50**, 675–702 (2004).

2. Crick, F. C. & Koch, C. What is the function of the claustrum? *Philosophical Transactions Royal Soc B Biological Sci* **360**, 1271–1279 (2005).

3. Fernández-Miranda, J. C., Rhoton, A. L., Kakizawa, Y., Choi, C. & Alvarez-Linera, J. The claustrum and its projection system in the human brain: a microsurgical and tractographic anatomical study. *J Neurosurg* **108**, 764–774 (2008).

4. Goll, Y., Atlan, G. & Citri, A. Attention: the claustrum. *Trends Neurosci* **38**, 486–495 (2015).

5. Kapakin, S. The claustrum: three-dimensional reconstruction, photorealistic imaging, and stereotactic approach. *Folia morphologica* **70**, 228–234 (2011).

6. Mathur, B. N., Caprioli, R. M. & Deutch, A. Y. Proteomic analysis illuminates a novel structural definition of the claustrum and insula. *Cereb Cortex* **19**, 2372–2379 (2009).

7. Milardi, D. *et al*. Cortical and subcortical connections of the human claustrum revealed in vivo by constrained spherical deconvolution tractography. *Cereb Cortex* **25**, 406–414 (2015).

8. Torgerson, C. M., Irimia, A., Goh, S. Y. M. & Horn, J. D. V. The DTI connectivity of the human claustrum. *Hum Brain Mapp* **36**, 827–838 (2015).

9. Qadir, H. *et al.* Structural Connectivity of the Anterior Cingulate Cortex, Claustrum, and the Anterior Insula of the Mouse. *Front Neuroanat* **12**, 100 (2018).

10. Banati, R. B., Goerres, G. W., Tjoa, C., Aggleton, J. P. & Grasby, P. The functional anatomy of visual-tactile integration in man: a study using positron emission tomography. *Neuropsychologia* **38**, 115–124 (2000).

11. Hadjikhani, N. & Roland, P. E. Cross-modal transfer of information between the tactile and the visual representations in the human brain: A positron emission tomographic study. *J Neurosci* **18**, 1072–1084 (1998).

12. Lerner, A. *et al*. Involvement of insula and cingulate cortices in control and suppression of natural urges. *Cereb Cortex* **19**, 218–223 (2009).

13. Naghavi, H. R., Eriksson, J., Larsson, A. & Nyberg, L. The claustrum/insula region integrates conceptually related sounds and pictures. *Neurosci Lett* **422**, 77–80 (2007).

14. Kalaitzakis, M. E., Pearce, R. K. B. & Gentleman, S. M. Clinical correlates of pathology in the claustrum in Parkinson's disease and dementia with Lewy bodies. *Neurosci Lett* **461**, 12–15 (2009).

15. Cascella, N. G., Gerner, G. J., Fieldstone, S. C., Sawa, A. & Schretlen, D. J. The insula-claustrum region and delusions in schizophrenia. *Schizophr Res* **133**, 77–81 (2011).

16. Cascella, N. G. & Sawa, A. The Claustrum. 237–243 (2014) doi:10.1016/b978-0-12-404566-8.00009-x.

17. Wada, J. A. & Kudo, T. Involvement of the claustrum in the convulsive evolution of temporal limbic seizure in feline amygdaloid kindling. *Electroencephalography and clinical neurophysiology* **103**, 249–256 (1997).

18. Heuvel, M. P. van den & Pol, H. E. H. Exploring the brain network: A review on resting-state fMRI functional connectivity. *Eur Neuropsychopharm* **20**, 519–534 (2010).

19. Krimmel, S. R. *et al.* Resting state functional connectivity and cognitive task-related activation of the human claustrum. *Neuroimage* **196**, 59–67 (2019).

20. Glasser, M. F. *et al.* The minimal preprocessing pipelines for the Human Connectome Project. *Neuroimage* **80**, 105–124 (2013).

21. Smith, S. M. *et al.* Resting-state fMRI in the Human Connectome Project. *Neuroimage* **80**, 144–68 (2013).

22. Essen, D. C. V. *et al.* The Human Connectome Project: a data acquisition perspective. *Neuroimage* **62**, 2222–2231 (2012).

23. Essen, D. C. V. *et al.* The WU-Minn Human Connectome Project: An overview. *Neuroimage* **80**, 62–79 (2013).

24. Ugurbil, K. *et al.* Pushing spatial and temporal resolution for functional and diffusion MRI in the Human Connectome Project. *Neuroimage* **80**, 80–104 (2013).

25. Whitfield-Gabrieli, S. & Nieto-Castañón, A. Conn: A Functional Connectivity Toolbox for Correlated and Anticorrelated Brain Networks. *Brain Connectivity* **2**, 125–141 (2012).

26. Friston, K. J., Jezzard, P. & Turner, R. Analysis of functional MRI time□series. *Hum Brain Mapp* **1**, 153–171 (1994).

27. Pirone, A. *et al.* Topography of Gng2- and NetrinG2-expression suggests an insular origin of the human claustrum. *Plos One* **7**, e44745 (2012).

28. Remedios, R., Logothetis, N. K. & Kayser, C. A role of the claustrum in auditory scene analysis by reflecting sensory change. *Frontiers Syst Neurosci* **8**, 44 (2014).

29. Volz, K. G., Schooler, L. J. & Cramon, D. Y. von. It just felt right: the neural correlates of the fluency heuristic. *Conscious Cogn* **19**, 829–837 (2010).

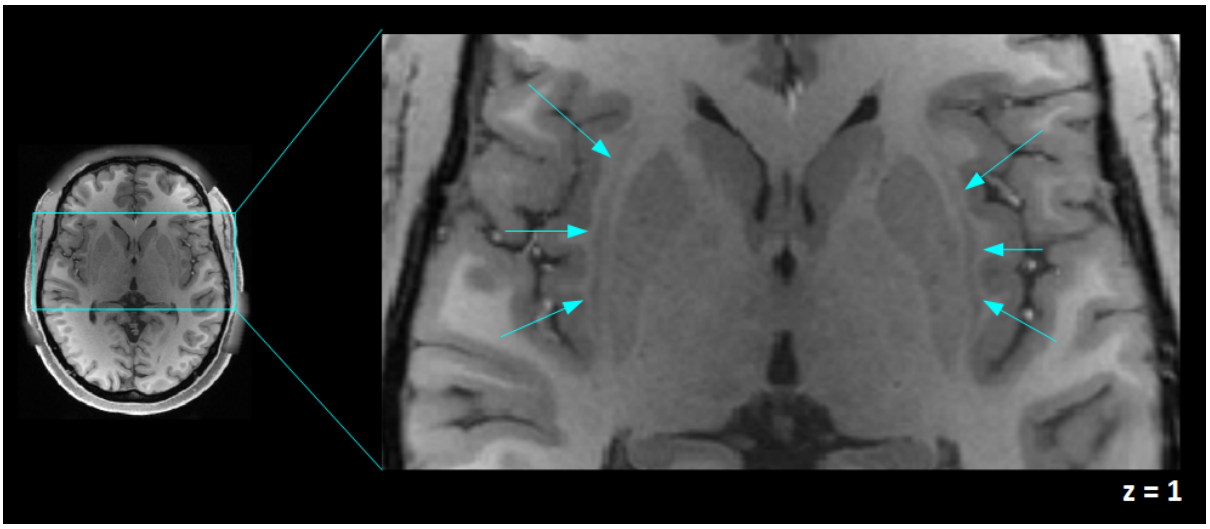

Figure 1. An axial view of the human claustrum. The human claustra are shown (signaled by blue arrows) between the external and extreme capsule, left and right claustra in a T1-weighted image of one of the participants are shown in MNI coordinates.

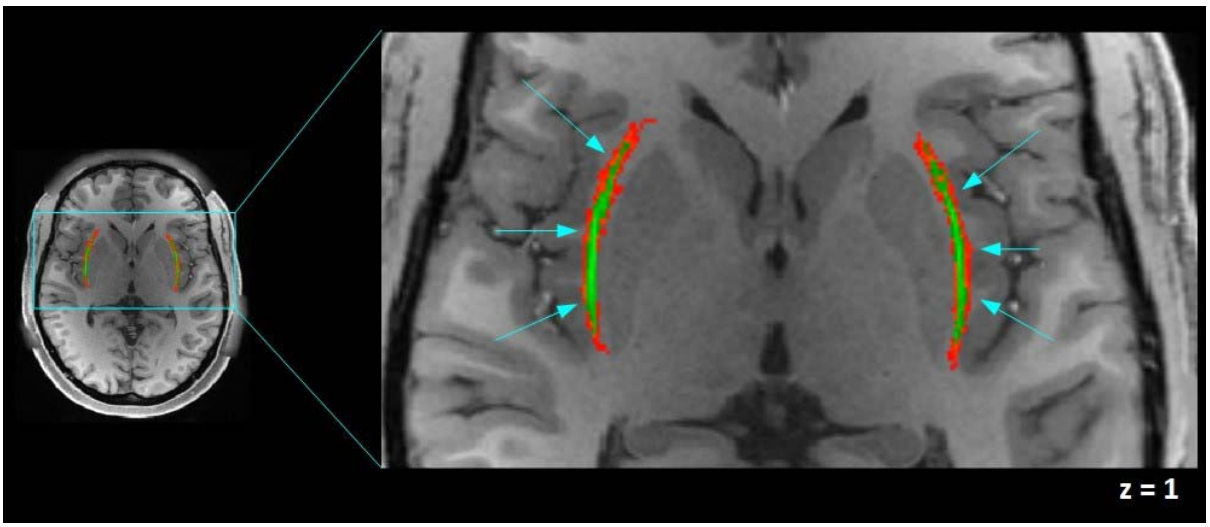

Figure 2. On an axial view, the averaged mask of the claustrum is shown in green, left and right claustra mask on a T1-weighted image of one of the participants are shown in MNI coordinates. In green, our effective claustrum ROI, was estimated from the intersection of all subjects´ claustrum. In red, variability area due to subject differences. In our analysis we include only the green area.

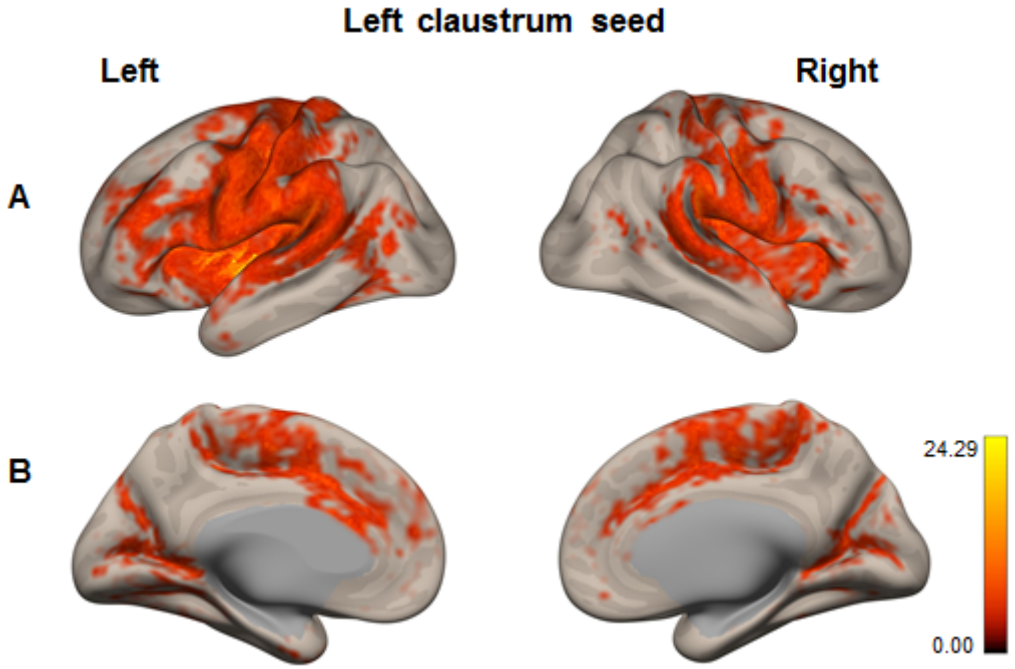

Figure 3. Seed-to-voxel functional connectivity with left claustrum as seed. ($p<0.05$, p-FDR corrected) Row (A) Left, Insular cortex, temporal cortex, precentral gyrus, postcentral gyrus, supramarginal gyrus, opercular cortex, frontal cortex. Right, insular cortex, precentral and postcentral gyrus, supramarignal gyrus, temporal cortex. (B) Left and right, cingulate gyrus (anterior division), occipital cortex.

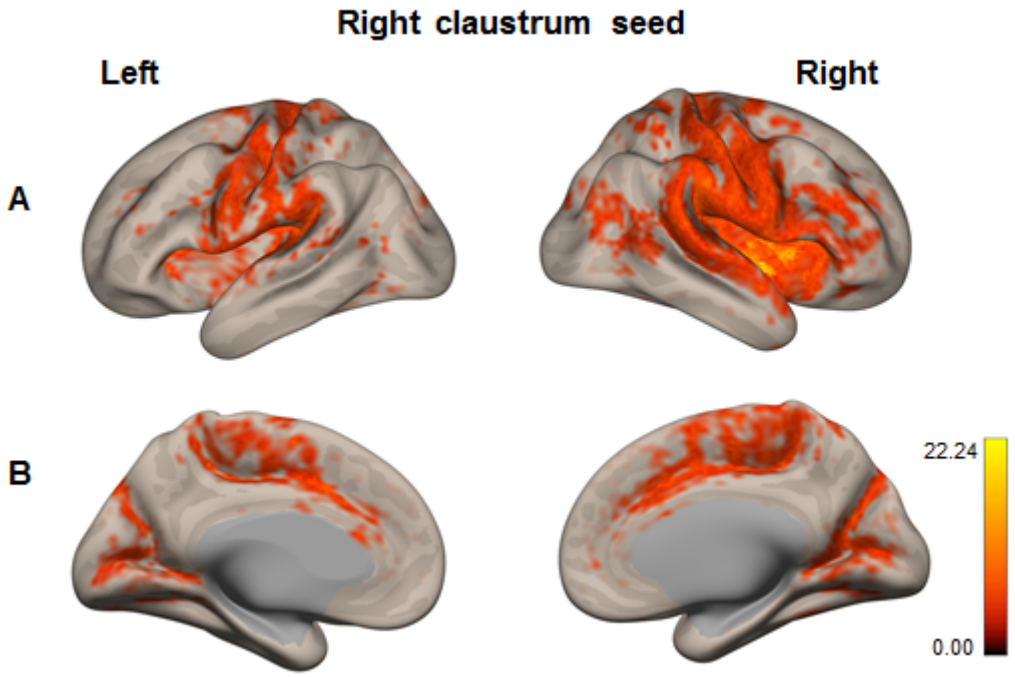

Figure 4. Seed-to-voxel functional connectivity with right claustrum as seed. ($p<0.05$, p-FDR corrected) Row (A) Left, precentral gyrus, postcentral gyrus. Right, insular cortex, precentral and postcentral gyrus, supramarginal gyrus, temporal cortex, frontal cortex. (B) Left, occipital cortex. Right, anterior cingulate cortex, occipital cortex.

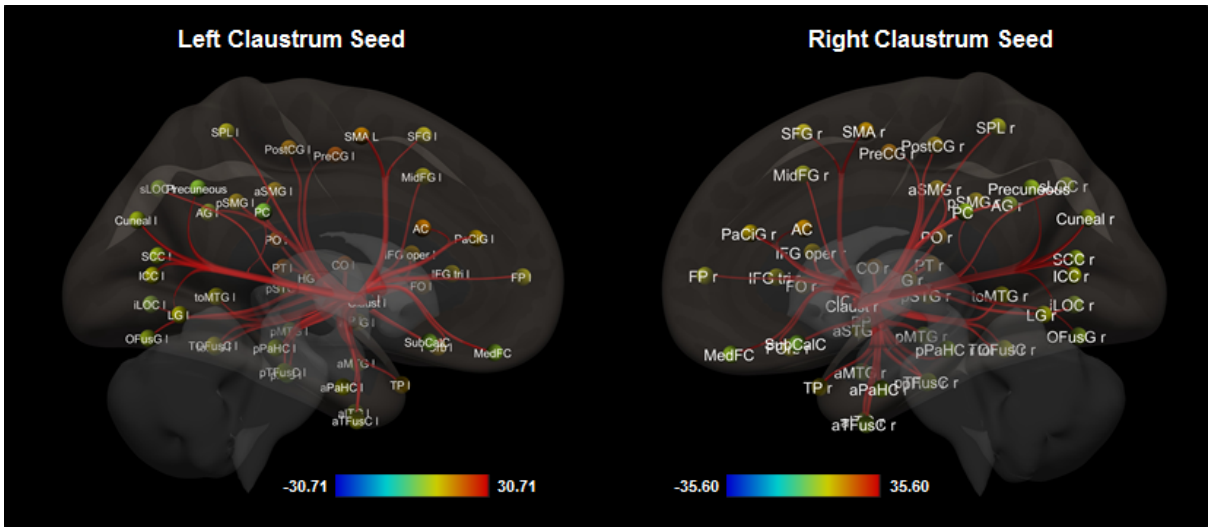

Figure 5. Seed-to-ROI functional positive connectivity between the claustra as seed and cortical ROIs. Left Calustrum seed show functional connectivity mainly with left insular cortex (IC), left opercular

cortex (CO), left precentral gyrus (PreCG), left planum temporale (PT), left and right supplementary motor area (SMA). Right Claustrum seed, mainly connected with right insular cortex (IC), right opercuar cortex (CO), right precentral gyrus (PreCG), right Heschl´s gyrus (HG), anterior cingulate cortex (AC), left and right supplementary motor area (SMA). The results are thresholded (p< 0.05, p-FDR corrected).

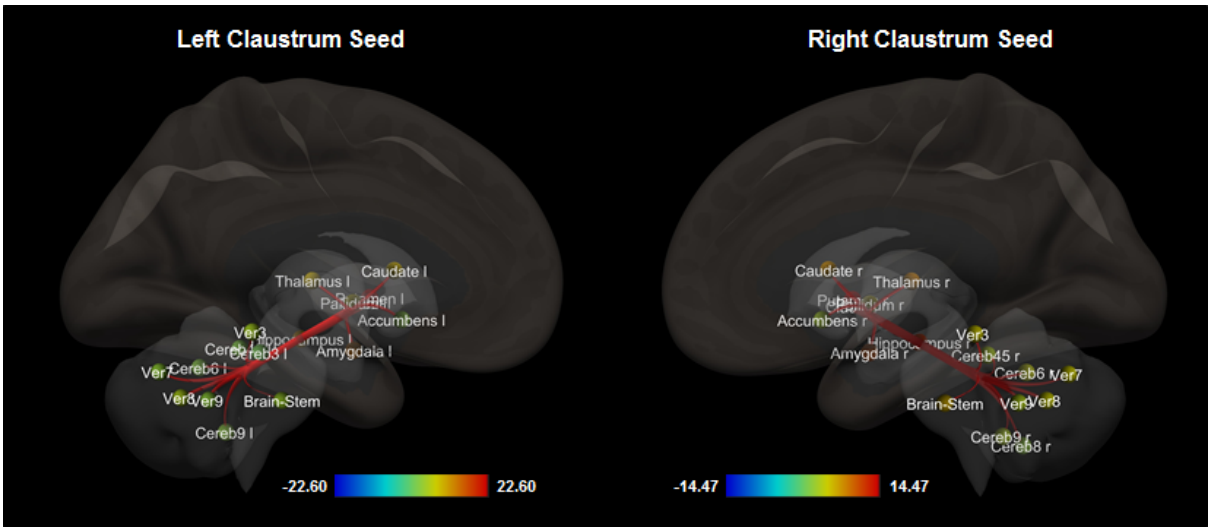

Figure 6. Seed-to-ROI functional positive connectivity between the claustra as seed and subcortical ROIs. Left claustrum seed is functionally connected with left and right putamen, left hippocampus, left amygdala, left and right caudate and cerebelar areas. Right claustrum seed show funcional connectivity with right putamen, right hippocampus, right amygdala, left putamen and cerebelar areas. The results are thresholded (p< 0.05, p-FDR corrected).

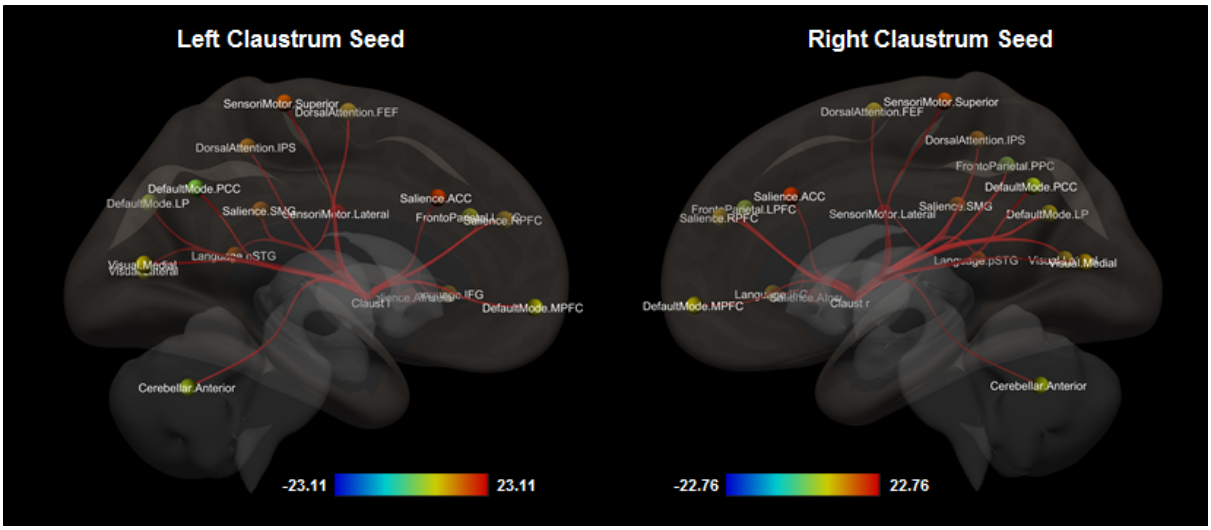

Figure 7. Seed-to-ROI functional positive connectivity between the claustra as seed and network´s nodes as ROIs. Left and right seed claustra, mainly connected with salience network nodes, such as anterior insular cortex, anterior cingulate cortex, supramarginal gyrus; sensorimotor network lateral and superior nodes; language network superior temporal gyrus and cerebellar anterior network. The results are thresholded (p< 0.05, p-FDR corrected).

TABLE I Left claustrum resting-state functional connectivity (cortical areas as ROIs)

Seed	Target (ROI)	beta	T(99)	p-FDR
Left Claustrum	Insular Cortex (IC) l	0.35	30.71	0.000000
	Central Opercular Cortex (CO) l	0.26	23.12	0.000000
	Precentral Gyrus (PreCG) l	0.25	22.51	0.000000
	Parietal Operculum (PO) l	0.25	21.14	0.000000
	Insular Cortex (IC) r	0.25	20.56	0.000000
	Planum Temporale (PT) l	0.24	20.41	0.000000
	Frontal Operculum Cortex (FO) l	0.21	20.17	0.000000
	Central Opercular Cortex (CO) r	0.22	20.16	0.000000
	Heschl's Gyrus (HG) l	0.22	20.01	0.000000
	SMA r	0.21	19.78	0.000000
	Planum Polare (PP) l	0.22	19.14	0.000000
	Anterior Cingulate Cortex (AC)	0.21	19.13	0.000000
	SMA l	0.20	19.00	0.000000
	Parietal Operculum (PO) r	0.21	18.90	0.000000
	Precentral Gyrus (PreCG) r	0.20	17.56	0.000000
	Planum Temporale (PT) r	0.21	17.49	0.000000
	Frontal Opeculum cortex (FO) r	0.17	17.35	0.000000
	Paracingulate Gyrus (PaCiG) l	0.17	17.08	0.000000
	Inferior Frontal Gyrus, (IFG oper) l	0.18	16.93	0.000000
	Frontal Orbital Cortex (FOrb) l	0.17	16.85	0.000000
	Postcentral Gyrus (PostCG) l	0.20	16.75	0.000000
	Heschl's Gyrus (HG) r	0.19	16.02	0.000000
	Supramarginal Gyrus, a (aSMG) l	0.17	16.01	0.000000
	Paracingulate Gyrus (PaCiG) r	0.14	15.81	0.000000
	Temporal Pole (TP) l	0.17	15.67	0.000000
	Superior Temporal Gyrus, a (aSTG) l	0.16	15.20	0.000000
	Supramarginal Gyrus, a (aSMG) r	0.15	14.77	0.000000
	Planum Polare (PP) r	0.14	14.31	0.000000
	Inferior Frontal Gyrus, (IFG oper) r	0.14	14.07	0.000000
	Parahippocampal Gyrus, a (aPaHC) l	0.12	13.92	0.000000
	Supramarginal Gyrus, p (pSMG) l	0.16	13.86	0.000000
	Superior Temporal Gyrus, p (pSTG) l	0.16	13.76	0.000000
	Inferior Frontal Gyrus, (IFG tri) l	0.15	13.72	0.000000
	Superior Temporal Gyrus, p (pSTG) r	0.15	13.39	0.000000
	Postcentral Gyrus Right (PostCG) r	0.15	13.17	0.000000
	Temporal Fusiform Cortex, a (aTFusC) l	0.11	13.06	0.000000
	Superior Frontal Gyrus (SFG) r	0.13	12.87	0.000000
	Middle Frontal Gyrus (MidFG) l	0.13	12.69	0.000000
	Inferior Frontal Gyrus (IFG tri) r	0.11	11.51	0.000000
	Frontal Pole (FP) l	0.12	11.34	0.000000
	Superior Frontal Gyrus (SFG) l	0.13	11.31	0.000000
	Supramarginal Gyrus, p (pSMG) r	0.11	10.45	0.000000
	Intracalcarine Cortex Right (ICC) l	0.12	10.38	0.000000
	Temporal Occipital Fusiform Cortex (TOFusC) l	0.13	10.15	0.000000
	Lingual Gyrus (LG) l	0.12	10.12	0.000000
	Frontal Orbital Cortex (FOrb) r	0.09	10.07	0.000000
	Superior Parietal Lobule (SPL) l	0.12	9.89	0.000000
	Middle Temporal Gyrus, temporooccipital part (toMTG) l	0.12	9.69	0.000000
	Temporal Pole (TP) r	0.11	9.56	0.000000

Superior Temporal Gyrus, a (aSTG) r	0.11	9.40	0.000000
Inferior Temporal Gyrus, a (aITG) l	0.09	9.27	0.000000
Lingual Gyrus (LG) r	0.10	9.14	0.000000
Middle Temporal Gyrus, a (aMTG) l	0.10	9.06	0.000000
Intracalcarine Cortex (ICC) r	0.11	8.82	0.000000
Parahippocampal Gyrus, p (pPaHC) l	0.08	8.77	0.000000
Temporal Fusiform Cortex, p (pTFusC) l	0.08	8.12	0.000000
Supracalcarine Cortex (SCC) l	0.08	8.06	0.000000
Angular Gyrus (AG) l	0.09	7.97	0.000000
Cuneal l	0.09	7.40	0.000000
Inferior Temporal Gyrus, a (aITG) r	0.06	7.25	0.000000
Temporal Occipital Fusiform Cortex (TOFusC) r	0.09	7.15	0.000000
Middle Temporal Gyrus, p (pMTG) l	0.08	7.03	0.000000
Occipital Fusiform Gyrus (OFusG) l	0.08	6.97	0.000000
Middle Temporal Gyrus, temporooccipital part (toMTG) r	0.08	6.94	0.000000
Cuneal r	0.09	6.79	0.000000
Supracalcarine Cortex (SCC) r	0.08	6.55	0.000000
Temporal Fusiform Cortex, p (pTFusC) r	0.06	6.45	0.000000
Subcallosal Cortex SubCalC	0.05	6.30	0.000000
Frontal Pole (FP) r	0.06	6.25	0.000000
Frontal Medial Cortex (MedFC)	0.06	6.02	0.000000
Superior Parietal Lobule (SPL) r	0.07	5.81	0.000000
Parahippocampal Gyrus, a (aPaHC) r	0.05	5.78	0.000000
Temporal Fusiform Cortex, a (aTFusC) r	0.05	5.68	0.000000
Occipital Fusiform Gyrus (OFusG) r	0.07	5.22	0.000001
Middle Frontal Gyrus (MidFG) r	0.05	5.16	0.000001
Middle Temporal Gyrus, p (pMTG) r	0.05	4.92	0.000003
Precuneous	0.05	4.91	0.000003
Inferior Temporal Gyrus, p (pITG) l	0.04	4.85	0.000003
Parahippocampal Gyrus, p (pPaHC) r	0.05	4.80	0.000004
Middle Temporal Gyrus, a (aMTG) r	0.05	4.73	0.000005
Lateral Occipital Cortex, i (iLOC) l	0.06	4.69	0.000006
Lateral Occipital Cortex, s (sLOC) l	0.06	4.69	0.000006
Cingulate Gyrus, p (PC)	0.05	4.67	0.000007
Inferior Temporal Gyrus, temporooccipital part (toITG) l	0.04	3.93	0.000104
Lateral Occipital Cortex, i (iLOC) r	0.04	3.30	0.000829
Angular Gyrus (AG) r	0.03	2.96	0.002366
Inferior Temporal Gyrus, temporooccipital part (toITG) r	0.03	2.64	0.005907
Lateral Occipital Cortex, s (sLOC) r	0.03	2.64	0.016127
Inferior Temporal Gyrus, p (pITG) r	0.01	1.70	0.052987

The results were corrected at seed level correction $p<0.05$ using False Discovery Rate (FDR). r = right, l = left, a = anterior division, p = posterior division, oper = pars opercularis, tri = pars triangularis, i = inferior, s = superior

TABLE II Right claustrum resting-state functional connectivity (cortical areas as ROIs)

Seed	Target (ROI)	beta	T(99)	p-FDR
Right Claustrum	Insular Cortex (IC) r	0.38	35.60	0.000000
	Frontal Operculum Cortex (FO) r	0.19	23.07	0.000000
	Central Opercular Cortex (CO) r	0.23	22.34	0.000000
	Precentral Gyrus (PreCG) r	0.22	21.83	0.000000
	Parietal Operculum (PO) r	0.21	21.64	0.000000
	Heschl's Gyrus (HG) r	0.20	20.85	0.000000
	Anterior Cingulate Cortex (AC)	0.20	19.95	0.000000
	Planum Temporale (PT) r	0.21	19.59	0.000000
	Planum Polare (PP) r	0.18	19.30	0.000000
	SMA r	0.19	18.63	0.000000
	Precentral Gyrus (PreCG) l	0.19	18.54	0.000000
	Supramarginal Gyrus, a (aSMG) r	0.17	18.46	0.000000
	Insular Cortex (IC) l	0.20	18.36	0.000000
	Planum Temporale (PT) l	0.17	17.77	0.000000
	Heschl's Gyrus (HG) l	0.16	17.51	0.000000
	Parietal Operculum (PO) l	0.17	17.48	0.000000
	Planum Polare (PP) l	0.16	17.43	0.000000
	SMA l	0.16	17.04	0.000000
	Inferior Frontal Gyrus, (IFG oper) r	0.16	16.90	0.000000
	Postcentral Gyrus (PostCG) r	0.17	16.82	0.000000
	Paracingulate Gyrus (PaCiG) r	0.16	16.53	0.000000
	Central Opercular Cortex (CO) l	0.17	15.92	0.000000
	Supramarginal Gyrus, (pSMG) r	0.15	15.55	0.000000
	Superior Frontal Gyrus (SFG) r	0.14	14.70	0.000000
	Superior Temporal Gyrus, p (pSTG) r	0.16	14.70	0.000000
	Frontal Opeculum cortex (FO) l	0.13	14.38	0.000000
	Temporal Pole (TP) r	0.15	14.18	0.000000
	Inferior Frontal Gyrus, (IFG tri) r	0.14	13.63	0.000000
	Superior Temporal Gyrus, a (aSTG) r	0.14	13.51	0.000000
	Frontal Orbital Cortex (FOrb) r	0.13	13.45	0.000000
	Postcentral Gyrus (PostCG) l	0.14	13.04	0.000000
	Middle Frontal Gyrus (MidFG) r	0.11	12.53	0.000000
	Paracingulate Gyrus (PaCiG) l	0.12	12.26	0.000000
	Superior Parietal Lobule (SPL) r	0.11	12.07	0.000000
	Supramarginal Gyrus, a (aSMG) l	0.11	11.94	0.000000
	Frontal Pole (FP) r	0.11	11.77	0.000000
	Intracalcarine Cortex Right (ICC) r	0.11	11.37	0.000000
	Lingual Gyrus (LG) r	0.12	11.10	0.000000
	Superior Temporal Gyrus, a (aSTG) l	0.10	10.90	0.000000
	Intracalcarine Cortex (ICC) l	0.11	10.82	0.000000
	Parahippocampal Gyrus, a (aPaHC) r	0.08	10.62	0.000000
	Frontal Orbital Cortex (FOrb) l	0.10	10.49	0.000000
	Temporal Occipital Fusiform Cortex Left (TOFusC) r	0.12	10.49	0.000000
	Temporal Fusiform Cortex, p (pTFusC) r	0.09	10.39	0.000000
	Temporal Occipital Fusiform Cortex Left (TOFusC) l	0.10	10.20	0.000000
	Inferior Frontal Gyrus, (IFG oper) l	0.10	10.16	0.000000
	Middle Temporal Gyrus, temporooccipital part (toMTG) r	0.12	9.87	0.000000
	Superior Temporal Gyrus, p (pSTG) l	0.10	9.86	0.000000

Supramarginal Gyrus, p (pSMG) l	0.09	9.68	0.000000
Inferior Temporal Gyrus, a (aITG) r	0.08	9.44	0.000000
Temporal Fusiform Cortex, p (pTFusC) l	0.08	9.40	0.000000
Cuneal r	0.10	9.26	0.000000
Lingual Gyrus (LG) l	0.10	9.11	0.000000
Cuneal l	0.09	9.06	0.000000
Parahippocampal Gyrus, p (pPaHC) l	0.07	8.95	0.000000
Supracalcarine Cortex (SCC) r	0.09	8.81	0.000000
Parahippocampal Gyrus, a (aPaHC) l	0.07	8.72	0.000000
Temporal Pole (TP) l	0.09	8.69	0.000000
Parahippocampal Gyrus, p (pPaHC) r	0.07	8.53	0.000000
Middle Temporal Gyrus, p (pMTG) r	0.09	8.49	0.000000
Precuneous	0.08	8.48	0.000000
Superior Parietal Lobule (SPL) l	0.09	8.46	0.000000
Temporal Fusiform Cortex, a (aTFusC) r	0.08	8.36	0.000000
Inferior Frontal Gyrus, (IFG tri) l	0.07	8.07	0.000000
Supracalcarine Cortex (SCC) l	0.08	7.92	0.000000
Superior Frontal Gyrus (SFG) l	0.08	7.82	0.000000
Cingulate Gyrus, p (PC)	0.07	7.78	0.000000
Angular Gyrus (AG) r	0.08	7.76	0.000000
Middle Temporal Gyrus, a (aMTG) r	0.07	7.74	0.000000
Lateral Occipital Cortex, s (sLOC) r	0.09	7.34	0.000000
Temporal Fusiform Cortex, a (aTFusC) l	0.05	7.31	0.000000
Occipital Fusiform Gyrus (OFusG)r	0.08	7.07	0.000000
Middle Frontal Gyrus (MidFG) l	0.07	6.91	0.000000
Frontal Medial Cortex (MedFC)	0.07	6.78	0.000000
Subcallosal Cortex (SubCalC)	0.05	6.66	0.000000
Inferior Temporal Gyrus, temporooccipital part (toITG) r	0.08	6.63	0.000000
Inferior Temporal Gyrus, p (pITG) r	0.06	6.57	0.000000
Lateral Occipital Cortex, i (iLOC) r	0.08	6.53	0.000000
Frontal Pole (FP) l	0.06	6.50	0.000000
Occipital Fusiform Gyrus (OFusG) l	0.07	6.47	0.000000
Middle Temporal Gyrus, temporooccipital part (toMTG) l	0.05	5.12	0.000001
Lateral Occipital Cortex, s (sLOC) l	0.05	4.16	0.000044
Lateral Occipital Cortex, i (iLOC) l	0.05	4.02	0.000070
Angular Gyrus (AG) l	0.04	3.84	0.000132
Middle Temporal Gyrus, a (aMTG) l	0.03	3.77	0.000167
Inferior Temporal Gyrus, a (aITG) l	0.03	3.54	0.000371
Middle Temporal Gyrus, p (pMTG) l	0.02	2.51	0.008046
Inferior Temporal Gyrus, temporooccipital part (toITG) l	0.02	2.40	0.010478

The results were corrected at seed level correction $p<0.05$ using False Discovery Rate (FDR). r = right, l = left, a = anterior division, p = posterior division, oper = pars opercularis, tri = pars triangularis, i = inferior, s = superior

TABLE III Left claustrum resting-state functional connectivity (subcortical areas as ROIs)

Seed	Target (ROI)	beta	T(99)	p-FDR
Left Claustrum	Putamen l	0.25	22.60	0.000000
	Putamen r	0.16	14.71	0.000000
	Hippocampus l	0.14	13.90	0.000000
	Amygdala l	0.16	13.63	0.000000
	Caudate r	0.10	11.64	0.000000
	Caudate l	0.11	11.61	0.000000
	Claustrum r	0.12	11.52	0.000000
	Pallidum l	0.09	9.92	0.000000
	Amygdala r	0.10	9.50	0.000000
	Thalamus l	0.11	9.45	0.000000
	Hippocampus r	0.09	9.14	0.000000
	Thalamus r	0.07	7.54	0.000000
	Pallidum r	0.04	4.67	0.000007
	Accumbens l	0.03	4.33	0.000023
	Accumbens r	0.02	2.57	0.006913

The results were corrected at seed level correction $p<0.05$ using False Discovery Rate (FDR).
l = left, r = right

TABLE IV Right claustrum resting-state functional connectivity (subcortical areas as ROIs)

Seed	Target (ROI)	beta	T(99)	p-FDR
Right Claustrum	Putamen r	0.15	14.47	0.000000
	Hippocampus r	0.13	13.26	0.000000
	Amygdala r	0.11	12.35	0.000000
	Putamen l	0.11	11.72	0.000000
	Claustrum l	0.12	11.52	0.000000
	Caudate l	0.08	10.36	0.000000
	Hippocampus l	0.09	10.26	0.000000
	Amygdala l	0.10	9.40	0.000000
	Thalamus r	0.09	9.10	0.000000
	Pallidum r	0.06	8.61	0.000000
	Caudate r	0.08	8.39	0.000000
	Brain-Stem	0.07	8.10	0.000000
	Thalamus l	0.07	7.54	0.000000
	Pallidum l	0.05	6.75	0.000000
	Accumbens l	0.03	5.06	0.000001
	Accumbens r	0.03	4.25	0.000031

The results were corrected at seed level correction $p<0.05$ using False Discovery Rate (FDR).
l = left, r = right

TABLE V Left claustrum resting-state functional connectivity (Cerebellar areas as ROIs)

Seed	Target (ROI)	beta	T(99)	p-FDR
Left Claustrum	Vermis 3	0.05	5.83	0.000000
	Vermis 8	0.06	5.36	0.000000
	Vermis 7	0.04	3.48	0.000477
	Vermis 9	0.03	3.42	0.000572
	Cerebelum 9 r	0.03	3.40	0.000613
	Cerebelum 9 l	0.03	3.36	0.000703
	Cerebelum 6 r	0.04	3.09	0.001603
	Cerebelum 45 r	0.03	2.90	0.002786
	Cerebelum 45 l	0.03	2.57	0.006913
	Cerebelum 6 l	0.03	2.18	0.018275

The results were corrected at seed level correction $p<0.05$ using False Discovery Rate (FDR).

TABLE VI Right claustrum resting-state functional connectivity (Cerebellar areas as ROIs)

Seed	Target (ROI)	beta	T(99)	p-FDR
Right Claustrum	Vermis 3	0.05	6.75	0.000000
	Vermis 7	0.05	5.87	0.000000
	Vermis 8	0.05	5.40	0.000000
	Cerebelum r 6	0.05	4.77	0.000004
	Cerebelum r 45	0.04	4.08	0.000057
	Vermis 9	0.04	4.05	0.000064
	Cerebelum l 9	0.04	3.90	0.000108
	Cerebelum r 9	0.03	3.66	0.000250
	Cerebelum l 6	0.03	3.05	0.001753
	Cerebelum l 45	0.02	2.58	0.006571
	Cerebelum l 3	0.02	2.40	0.010533
	Cerebelum l 8	0.02	2.31	0.012909
	Cerebelum r 8	0.02	2.03	0.025289

The results were corrected at seed level correction $p<0.05$ using False Discovery Rate (FDR).

TABLE VII Left claustrum resting-state functional connectivity (network´s nodes as ROIs)

Seed	Target (ROI)	beta	T(99)	p-FDR
Left Claustrum	A Insula l (Salience)	0.24	23.11	0.000000
	Sensorimotor lateral l	0.24	21.86	0.000000
	A Insula r (Salience)	0.19	19.39	0.000000
	Sensorimotor lateral r	0.20	18.39	0.000000
	Anterior Cingulate Cortex (ACC) (Salience)	0.19	18.04	0.000000
	Supramarginal Gyrus (SMG) l (Salience)	0.16	17.06	0.000000
	Sensorimotor superior	0.17	15.02	0.000000
	Supramarginal Gyrus (SMG) r (Salience)	0.13	14.20	0.000000
	Rostral Prefrontal Cortex (RPFC) l (Salience)	0.13	13.70	0.000000
	Superior Temporal Gyrus (pSTG) l (Language)	0.17	13.46	0.000000
	Frontal Eye Field (FEF) l (Dorsal-Attention)	0.12	13.23	0.000000
	Inferior Frontal Gyrus (IFG) l (Language)	0.13	12.90	0.000000
	IntraParietal Sulcus (IPS) l (Dorsal-Attention)	0.15	12.42	0.000000
	Posterior Superior Temporal Gyrus (pSTG) r (Language)	0.13	11.01	0.000000
	Inferior Frontal Gyrus (IFG) r (Language)	0.10	9.99	0.000000
	Frontal Eye Field (FEF) r (Dorsal-Attention)	0.08	9.14	0.000000
	Rostral Prefrontal Cortex (RPFC) r (Salience)	0.07	8.33	0.000000
	IntraParietal Sulcus (IPS) r (Dorsal-Attention)	0.10	7.95	0.000000
	Visual Medial	0.09	7.85	0.000000
	Medial Prefrontal Cortex (MPFC) (Default Mode)	0.08	7.67	0.000000
	Lateral Prefrontal Cortex (LPFC) l (Fronto-Parietal)	0.08	7.56	0.000000
	Visual Lateral l	0.08	6.25	0.000000
	Cerebellar Anterior	0.06	4.66	0.000007
	Visual Lateral r	0.06	4.50	0.000012
	Lateral Parietal (LP) l (Default Mode)	0.05	4.25	0.000032
	Lateral Parietal (LP) r (Default Mode)	0.04	3.63	0.000296

The results were corrected at seed level correction $p<0.05$ using False Discovery Rate (FDR).
l = left, r = right

TABLE VIII Right claustrum resting-state functional connectivity (network´s nodes as ROIs)

Seed	Target (ROI)	beta	T(99)	p-FDR
Right Claustrum	AInsula r (Salience)	0.21	22.76	0.000000
	Sensoriomotor lateral r	0.21	19.58	0.000000
	Anterior Cingulate Cortex (ACC) (Salience)	0.18	19.44	0.000000
	AInsula l (Salience)	0.16	17.52	0.000000
	Sensoriomotor lateral l	0.17	16.45	0.000000
	Supramarginal Gyrus (SMG) r (Salience)	0.14	16.22	0.000000
	Sensorimotor superior	0.15	15.04	0.000000
	Rostral Prefrontal Cortex (RPFC) r (Salience)	0.10	14.48	0.000000
	Posterior Superior Temporal Gyrus pSTG r (Language)	0.15	14.29	0.000000
	IntraParietal Sulcus (IPS) r (Dorsal-Attention)	0.13	13.80	0.000000
	Frontal Eye Field (FEF) l (Dorsal-Attention)	0.09	12.20	0.000000
	Supramarginal Gyrus (SMG) l (Salience)	0.10	11.33	0.000000
	Frontal Eye Field (FEF) r (Dorsal-Attention)	0.09	10.89	0.000000
	Inferior Frontal Gyrus (IFG) r (Language)	0.10	10.43	0.000000
	Intraparietal Sulcus (IPS) l (Dorsal-Attention)	0.10	10.16	0.000000
	Visual Medial	0.10	9.26	0.000000
	Rostral Prefrontal Cortex (RPFC) l (Salience)	0.08	9.23	0.000000
	Posterior Superior Temporal Gyrus (pSTG) l (Language)	0.09	8.64	0.000000
	Visual Lateral r	0.10	8.49	0.000000
	Medial Prefrontal Cortex (MPFC) (Default Mode)	0.08	8.07	0.000000
	Lateral Parietal (LP) r (Default Mode)	0.08	8.03	0.000000
	Visual Lateral l	0.07	6.63	0.000000
	Precuneus Cortex (PCC) (Default Mode)	0.05	5.68	0.000000
	Cerebellar Anterior	0.06	5.67	0.000000
	Inferior Frontal Gyrus (IFG) l (Language)	0.05	5.25	0.000001
	Lateral Prefrontal Cortex (LPFC) r (Frontoparietal)	0.05	5.09	0.000001
	Lateral Prefrontal Cortex (LPFC) l (Frontoparietal)	0.04	4.97	0.000002
	Posterior Parietal Cortex (PPC) r (Frontoparietal)	0.03	3.23	0.000989
	Lateral Parietal (LP) l (DefaultMode)	0.02	2.66	0.005425

The results were corrected at seed level correction $p<0.05$ using False Discovery Rate (FDR).
l = left, r = right